A Frequency Dependent Solution for Microstrip Transmission Lines

EDGAR J. DENLINGER, MEMBER, IEEE

Abstract—Theoretical and experimental results of "open" microstrip propagation on both a pure dielectric and a demagnetized ferrite substrate are presented. The theory enables one to obtain the frequency dependence of phase velocity and characteristic impedance, and also to obtain the electromagnetic field quantities around the microstrip line. It utilizes a Fourier transform method in which the hybrid-mode solutions for a "fictitious" surface current at the substrate–air interface are summed in such a way as to represent the fields caused by a current distribution that is finite only over the region occupied by the conducting strip and is assumed equal to that for the quasi-static case.

I. Introduction

MICROSTRIP is a very attractive transmission line for microwave integrated-circuit applications involving a large number of identical units and requiring a high density of packaging. The numerical solutions obtained thus far for the phase velocity and characteristic impedance of microstrip have been either quasi-static approximations, which assume a TEM mode of propagation [1]–[6], or analyses of a dielectric-loaded waveguide with a microstrip line, which assume a hybrid mode that is decomposed into LSE and LSM space harmonics [7]–[9]. The object of this paper is to present an approximate hybrid-mode solution that gives the frequency dependence of an open microstrip line deposited on either a dielectric or a demagnetized ferrite substrate.

Fig. 1 shows the physical construction of the microstrip line which is assumed to be completely lossless. The substrate is characterized by the relative dielectric constant K and the relative permeability μ_r. For the cases of a ceramic substrate and a demagnetized ferrite substrate, these two parameters are taken as isotropic scalar quantities. As will be shown later on, μ_r is a function of the frequency and the saturation magnetization of the ferrite. In this analysis the strip is assumed to have a negligibly small thickness.

The formulation of an exact theory for the microstrip structure is difficult because the cross section is not homogeneous. Furthermore, microstrip is an open structure where the energy is not confined to a finite region. Without the dielectric it would be a Lecher-type structure that could support a TEM mode. However, the presence of the dielectric allows the wave to be TEM only at zero frequency. For a simple grounded dielectric slab configuration subject to a physical field due to some arbitrary source, the complete solution consists of a discrete number of surface waves, a continuous spectrum of evanescent waves, and a continuous eigenvalue field, i.e., radiation field [10]. Leaky modes which correspond to a flow of power away from the surface do not satisfy the radiation conditions at infinity and thus do not belong to the proper eigenvalue spectrum [11]. Goubau shows that for the case of open waveguide structures, the radiation fields and the surface-wave fields are mathematically separable by orthogonality relations [12]. Therefore, the following theory for microstrip takes into account only the surface-wave fields. Due to boundary conditions involving transverse inhomogeneity in the dielectric and the presence of the strip, no pure TE or TM modes may exist. Thus, a hybrid-mode solution that can be expressed in terms of a complete set of simpler solutions having a z dependence of e^{-jkz} is sought. The proof of mode orthogonality for surface waveguides, as presented by Collin [11], enables a given arbitrary field to be expanded into a series of TE and TM modes. A linear combination of these modes is allowed for the case where the substrate's permeability and dielectric constant are both scalar quantities. The following gives the derivation of a hybrid mode of propagation.

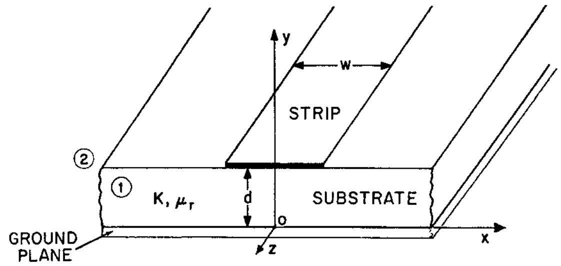

K relative dielectric constant of substrate
μ_r relative permeability of substrate
d substrate thickness
w strip width.

Fig. 1. Microstrip configuration.

II. Derivation of Electromagnetic Field Expressions

Two different analyses are presented here: one takes into account the presence of both a longitudinal and a transverse component of current on the strip and is, therefore, very lengthy; the other, which assumes the transverse current to be negligible, is more practical.

Manuscript received January 16, 1970; revised July 20, 1970.
This paper is part of a Ph.D. dissertation submitted to the University of Pennsylvania, Philadelphia, Pa.
The author is with the Lincoln Laboratory, Massachusetts Institute of Technology, Lexington, Mass.

A. Analysis for Both Longitudinal and Transverse Currents

The method of solution is to construct series of functions, each of which independently satisfies the wave equation for a TE mode or a TM mode and also satisfies boundary conditions on the ground plane and at infinity. Appropriate sets of functions are obtained by taking a Fourier transform of the fields along the x axis, which is oriented as shown by Fig. 1. The remaining boundary conditions on the strip and along the substrate–air interface are satisfied by the use of a linear combination of the TE- and TM-mode fields. A solution for the Fourier components of field is first obtained for a grounded dielectric (or ferrite) slab which does not possess a current-carrying strip. Instead, it has a "fictitious" surface current whose amplitude varies sinusoidally in the x direction along the substrate–air interface and has vector components both in the x and the z directions. The hybrid-mode fields that are caused by the actual current distribution, which is nonzero only over the region occupied by the strip, are found by taking a Fourier integral of the above sinusoidal components and are forced to satisfy the requirement that the tangential electric field vanish on the strip.

The Fourier transform method described above was used by Schetzen [13] in 1954 to obtain the fields which result from a uniform longitudinal current distribution on the strip. His theoretical analysis of a microstrip line on a pure dielectric substrate resulted in the invalid conclusion that the phase velocity is constant with frequency. From the Green's function static solution of Bryant and Weiss [3], it is clear that the current is not constant across the strip width. In fact, its amplitude increases very rapidly at the edges of the strip. In the hybrid-mode analysis the complete solution would treat the longitudinal and transverse current distributions as unknowns along with the propagation constant. This would result in a coupled pair of integral equations that would be extremely difficult to solve. A first-order solution is obtained here which estimates the frequency-dependent current distributions as being equal to that obtained under quasi-TEM conditions [14]. As long as the microstrip dimensions of strip width and substrate thickness are a small fraction of a wavelength, this approximation is considered good.

Without the substrate the TEM mode's longitudinal current distribution is related to the distribution of charge $\sigma(x)$ (which is obtained from capacitance calculations [3] with the potential on the strip set to unity) by the expression

$$I_z(x) = v\sigma(x), \qquad v = \text{phase velocity}.$$

This distribution remains the same for any nonmagnetic dielectric substrate. It is somewhat different for a demagnetized ferrite because of the discontinuity in the permeability at the substrate–air interface. For this case use can be made of the dual relationships existing

TABLE I

CURRENT DISTRIBUTION DATA—COMPARISON OF GREEN'S FUNCTION SOLUTION WITH THAT USING MAXWELL'S FUNCTION

	$I(m)$: $K=1$; $w/d=0.5$		$I(m)$: $K=15$; $w/d=0.5$	
m	Maxwell's Function	Green's Function	Maxwell's Function	Green's Function
1	0.5843	0.5836	0.5481×10	0.5474×10
2	0.5903	0.5895	0.5537	0.5529
3	0.6027	0.6020	0.5653	0.5644
4	0.6230	0.6223	0.5844	0.5831
5	0.6535	0.6530	0.6130	0.6115
6	0.6988	0.6989	0.6555	0.6539
7	0.7680	0.7692	0.7204	0.7190
8	0.8823	0.8893	0.8276	0.8302
9	1.1078	1.0800	1.0391	1.0070
10	1.8690	2.4490	1.7531	2.2800

Note: m is the number of elementary strip widths ($\Delta x/d=0.025$) from center of strip region ($x=0$).

for the electric and the magnetic fields of the microstrip [15]. The distribution of current can then be obtained by combining the above-mentioned dual relationships with the Green's function method of Bryant and Weiss. Because the permeability of a demagnetized ferrite [see (31)] is always close to one ($1>\mu_r>0.7$) over the frequency range for which losses are not excessive, the current distribution remains very close to that obtained with $K=1$, $\mu_r=1$. Therefore, in this paper, the same longitudinal current distribution is used for microstrip with both dielectric and demagnetized ferrite substrates. A closed-form expression was sought that would closely describe the numerical charge distribution data obtained by the quasi-static methods. The following relationship was derived by Maxwell for the charge density distribution on an isolated conducting strip [6], [16] (see Appendix for derivation):

$$\sigma(x) = \frac{\sigma_0}{\pi\sqrt{1-(2x/w)^2}}, \qquad -w/2 < x < w/2$$
$$= 0 \text{ otherwise.} \tag{1}$$

Table I illustrates how well this relationship agrees with the computed Green's function data [3] for two widely different substrate dielectric constants. It was found that changing the w/d ratio between 0.2 and 1.2 only affected the amplitude σ_0 without significantly changing the current's functional dependence on x. In the analysis to follow, use is made of the Fourier transform of $I_z(x)$. Therefore its amplitude I_{z0} is not needed in order to find the desired quantities of phase velocity and characteristic impedance. The Fourier transform of the current distribution is given by a zero-order Bessel function as shown below:

$$I_z(\alpha) = \frac{1}{2\pi}\int_{-\infty}^{\infty} I_z(x)e^{-j\alpha x}dx$$
$$= I_{z0}J_0(\alpha w/2). \tag{2}$$

It will be shown later that the use of this current function gives results that are in excellent agreement with experimental results and with the TEM solutions at zero frequency. However, the computations require excessive computer time. Another expression that was used by Yamashita [6] was found to give sufficient accuracy, and yet its Fourier transform allowed the computer time to be reduced by a factor of 5 (from two minutes to about twenty-four seconds per point):

$$I_z(x) = I_{z0}(1 + |2x/w|^3), \qquad |x| \leq w/2$$
$$= 0 \quad \text{otherwise.} \tag{3}$$

The Fourier transform of (3) is:

$$\tilde{I}_z(\alpha) = \frac{2I_{z0}}{\pi\alpha}\left\{\frac{24}{(\alpha w)^3} + \frac{3[(\alpha w)^2 - 8]}{(\alpha w)^3}\cos(\alpha w/2) + \frac{[(\alpha w)^2 - 12]}{(\alpha w)^2}\sin(\alpha w/2)\right\}. \tag{4}$$

Fig. 2 shows a comparison between the current distribution given by the above function and that calculated by the Green's function method. The effect of the lower $I_z(x)$ near the edge of the strip is to give a slightly lower value (less than one percent) for the microstrip line's effective dielectric constant.

In order to estimate the transverse component of current, the continuity equation is utilized to relate this quantity to the charge density distribution $\sigma(x)$ on the strip in the following manner (see Appendix):

$$\frac{\partial I_x(x)}{\partial x} = -j\omega[\sigma(x) - c\sigma_a(x)] \tag{5}$$

where ω is the angular frequency and c is the scaling factor relating the total charges on the strip with and without the substrate. Substitution of the charge data into the above equation results in a transverse current distribution of the form shown in Fig. 3. The following equations closely describe this current:

$$I_x(x) = I_{x0}\sin\frac{\pi x}{0.7w}, \qquad |x| \leq 0.8\frac{w}{2}$$
$$= I_{x0}\cos\frac{\pi x}{0.2w}, \qquad 0.8 < |x| \leq \frac{w}{2}. \tag{6}$$

Taking the Fourier transform of the above equation gives

$$\tilde{I}_x(\alpha) = I_{x0}\left[\frac{\sin G_1(\alpha)}{G_1(\alpha)} - \frac{\sin G_2(\alpha)}{G_2(\alpha)} + \frac{\cos 0.4G_3(\alpha) - \cos 0.5G_3(\alpha)}{G_3(\alpha)} + \frac{\cos 0.4G_4(\alpha) - \cos 0.5G_4(\alpha)}{G_4(\alpha)}\right] \tag{7}$$

where

$$G_1(\alpha),\, G_2(\alpha) = 0.4\left(\frac{\pi}{0.7} \mp \alpha w\right)$$
$$G_3(\alpha),\, G_4(\alpha) = \alpha w \mp 5\pi.$$

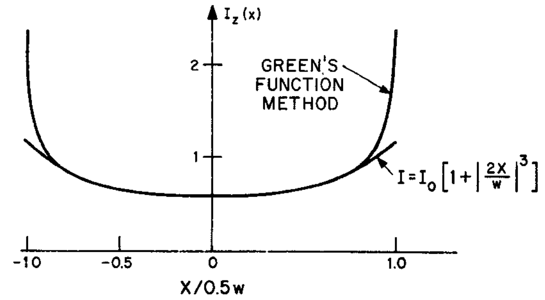

Fig. 2. Longitudinal current distribution on microstrip.

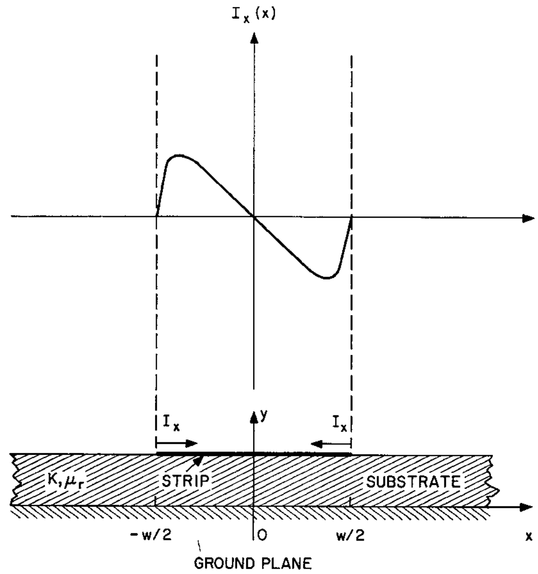

Fig. 3. Transverse current distribution on microstrip.

The electromagnetic field expressions to be derived are exact for the case of a sinusoidal surface current distribution flowing along the substrate–air interface, which does not possess a conducting strip. The solutions for an infinite number of these fictitious sinusoidal components are summed up in such a manner as to represent the fields caused by a current distribution that is finite only over the strip width w and equal to the static charge distribution. At this stage, the conducting strip is simply represented by a surface current over a finite region w. The introduction of the boundary condition that the tangential electric field be zero at ($y=d$, $|x| \leq w/2$) results from the strip being a perfect conductor.

The fictitious surface current flowing at the substrate–air interface generates a hybrid mode, which can be represented as a linear combination of TM and TE modes because these modes form a complete set in terms of which an arbitrary field can be represented. For a cylindrical structure of arbitrary cross section, the TM and TE modes may be derived from an electric-type Hertzian potential $\bar{\pi}_e = \bar{a}_z N\psi_e(x, y)e^{j(\omega t - kz)}$ and a magnetic Hertzian potential $\bar{\pi}_h = \bar{a}_z N\psi_h(x, y)e^{j(\omega t - kz)}$, respectively [17]. N is an arbitrary constant that is dependent upon the source strength, while the functions ψ_e and ψ_h both satisfy a two-dimensional scalar Helmholtz equation given below:

$$\nabla_t^2 \psi_{e,h} + \nu^2 \psi_{e,h} = 0 \tag{8}$$

where

$$\begin{aligned} \nu^2 = P_1^2 &= \omega^2 \mu_r K \mu_0 \epsilon_0 - k^2, \qquad y < d \\ = P_2^2 &= \omega^2 \mu_0 \epsilon_0 - k^2, \qquad y > d. \end{aligned}$$

Regions 1 and 2 are the substrate and air regions, respectively. The above potential functions can be written in terms of their Fourier transform $\psi(\alpha, y)$ with respect to x:

$$\psi(x, y) = \frac{1}{2\pi} \int_{-\infty}^{\infty} \psi(\alpha, y) e^{j\alpha x} d\alpha = \frac{1}{2\pi} \int_{-\infty}^{\infty} \phi \, d\alpha \tag{9}$$

where

$$\phi = \psi(\alpha, y) e^{j\alpha x}.$$

Combining (8) and (9) results in the following differential equations:

$$\begin{aligned} \left(\frac{d^2}{dy^2} + P_2^2 - \alpha^2\right) \begin{Bmatrix} \psi_e(\alpha, y) \\ \psi_h(\alpha, y) \end{Bmatrix} &= 0, \qquad y > d \\ \left(\frac{d^2}{dy^2} + P_1^2 - \alpha^2\right) \begin{Bmatrix} \psi_e(\alpha, y) \\ \psi_h(\alpha, y) \end{Bmatrix} &= 0, \qquad y < d. \end{aligned} \tag{10}$$

Since the total energy of the wave must be finite and the natural propagating modes for the grounded dielectric slab configuration are surface modes [10], the fields must decay exponentially with y in the air region ($y > d$). Therefore, the transverse wavenumber can be defined by

$$\beta_2 = (\alpha^2 - P_2^2)^{1/2}. \tag{11}$$

If radiation from the line is neglected, then β_2 will always be a real positive number as long as $k^2 > \omega^2 \mu_0 \epsilon_0$, which is true for a slow wave. Radiation from the microstrip [18] becomes significant only when the line is in the form of an open-circuited resonator or a disk cavity resonator and has a large normalized substrate thickness ($d/\lambda_0 > 0.01$) and/or a substrate of low dielectric constant ($K < 9$). The field components in the two regions ($i = 1, 2$) are obtained by means of the following equations [11]:

$$\begin{aligned} E_{zi} &= \frac{P_i^2}{jk} \psi_{ei}(x, y) \\ E_{ti} &= -\nabla_t \psi_{ei} + \frac{\omega \mu_i}{k} \bar{a}_z \times \nabla_t \psi_{hi} \\ H_{ti} &= -\frac{\omega K_i}{k} \bar{a}_z \times \nabla_t \psi_{ei} - \nabla_t \psi_{hi} \\ H_{zi} &= \frac{P_i^2}{jk} \psi_{hi}(x, y). \end{aligned} \tag{12}$$

The possible modes existing on the microstrip may be subdivided into the $\psi_{h\,\text{odd}}$–$\psi_{e\,\text{even}}$ and the $\psi_{e\,\text{odd}}$–$\psi_{h\,\text{even}}$ modes, the plane of even and odd symmetry being $x = 0$. The former corresponds to the fundamental mode for which the symmetry plane is a magnetic wall. It is considered to be a small perturbation from the pure TEM mode that would exist without the substrate and is of greatest interest. A solution for the higher order modes, namely the $\psi_{e\,\text{odd}}$–$\psi_{h\,\text{even}}$ modes, would proceed along the same steps except that the magnetic wall in the plane of symmetry is replaced by an electric wall. Since these modes are believed to be insignificant unless the microstrip dimensions are an appreciable fraction of a wavelength, the computations in this paper have been confined to the fundamental mode case.

The boundary conditions on the ground plane and at infinity as well as the symmetry around the plane $x = 0$ cause the fundamental mode's potential functions to have the form:

$$\begin{aligned} \phi_e &= \psi_e(\alpha, y) \cos \alpha x \\ \psi_e(\alpha, y) &= A_s \sin \beta_1 y, \qquad y < d \\ &= B_s \exp[-\beta_2(y - d)], \qquad y > d \\ \phi_h &= \psi_h(\alpha, y) \sin \alpha x \\ \psi_h(\alpha, y) &= C_s \cos \beta_1 y, \qquad y < d \\ &= D_s \exp[-\beta_2(y - d)], \qquad y > d \end{aligned} \tag{13}$$

where

$$\beta_1 = (P_1^2 - \alpha^2)^{1/2}. \tag{14}$$

The coefficients A_s, B_s, C_s, and D_s, and thus all the field expressions, can be determined from the following boundary conditions at the interface between the substrate (region 1) and the air (region 2):

$$\mathcal{E}_{z1} = \mathcal{E}_{z2} \tag{15}$$

$$\mathcal{E}_{x1} = \mathcal{E}_{x2} \tag{16}$$

$$\mathcal{H}_{z1} - \mathcal{H}_{z2} = -I_x(\alpha) \tag{17}$$

$$\mathcal{H}_{x1} - \mathcal{H}_{x2} = I_z(\alpha). \tag{18}$$

All the above field quantities are Fourier transforms with respect to x of the real fields. The boundary conditions lead to four simultaneous equations from which the coefficients of the potentials can be obtained in terms of the two components of current on the strip and the unknown propagation constant k. The expressions for the real field quantities can then be obtained by the use of (9), (12), and (13).

B. Analysis for Only Longitudinal Component of Current

As mentioned in the Appendix, the amplitude of the transverse current component is proportional to the normalized strip width w/λ, which for most applications is very small. When this parameter is less than 0.1, the transverse current is at least an order of magnitude smaller than the longitudinal current. Thus, a good approximation to the exact microstrip solution is to follow the same procedure as discussed in the previous section but to make I_x equal to zero. As a result, each of the coefficients of the potentials has only one term instead of two.

III. Derivation of Integral Equation for the Phase Velocity

This section contains derivations of the integral equations for obtaining the microstrip phase velocity. The same two cases involving the current components as were treated in Section II are considered here.

A. Solution for Both Longitudinal and Transverse Currents

In anticipation of a slow-wave type of solution for a lossless microstrip line, the axial propagation constant (jk) is taken to be a pure imaginary quantity and the value of k is expected to be in the range $k_0 \le k \le k_0 \sqrt{\mu_r K}$, where $k_0 = \omega\sqrt{\mu_0\epsilon_0}$. The quantity k along with the phase velocity v are of the form

$$k = \frac{2\pi}{\lambda_0}\sqrt{\xi}$$

$$v = v_0/\sqrt{\xi} \tag{19}$$

where

- v_0 velocity of light *in vacuo*
- λ_0 free-space wavelength
- ξ $\mu_{\text{eff}}\epsilon_{\text{eff}}$
- μ_{eff} effective relative permeability of microstrip line
- ϵ_{eff} effective relative dielectric constant of microstrip line.

ξ is found by using the following boundary conditions which result from the strip region being a perfect conductor:

$$E_{z2}(x, d) = 0, \tag{20}$$

$$\frac{dH_{z2}(x, d)}{dy} = 0, \qquad -w/2 \le x \le w/2. \tag{21}$$

Now, the total fields E_{z2} and H_{z2} are given by the following Fourier integral representations in terms of the coefficients B_s and D_s:

$$E_{z2}(x, y) = \int_{-\infty}^{\infty} \frac{P_2^2}{jk} B_s \cos\alpha x \exp\left[-\beta_2(y-d)\right]d\alpha \tag{22}$$

$$H_{z2}(x, y) = \int_{-\infty}^{\infty} \frac{P_2^2}{jk} D_s \sin\alpha x \exp\left[-\beta_2(y-d)\right]d\alpha. \tag{23}$$

These expressions describe the longitudinal fields caused by the actual current distribution, which is nonzero only over the region occupied by the strip. Use of the relations for B_s and D_s and (20)–(23) results in a coupled pair of integral equations involving the two current components:

$$I_{x0}\int_{-\infty}^{\infty} \frac{j}{\det}\left[F_1 b_{22} + \frac{k\alpha}{P_1^2} b_{12}\right] I_x(\alpha)\cos\alpha x\, d\alpha - I_{z0}\int_{-\infty}^{\infty} \frac{b_{12}}{\det} I_z(\alpha)\cos\alpha x\, d\alpha = 0$$

$$I_{x0}\int_{-\infty}^{\infty} \frac{j\beta_2}{\det}\left[\frac{k\alpha}{P_1^2} b_{11} - F_1 b_{21}\right] I_x(\alpha)\sin\alpha x\, d\alpha - I_{z0}\int_{-\infty}^{\infty} \frac{\beta_2 b_{11}}{\det} I_z(\alpha)\sin\alpha x\, d\alpha = 0 \tag{24}$$

where x lies within the strip region $|x| \le w/2$ and

$$b_{11} = -b_{22} = \alpha\left[\left(\frac{P_2}{P_1}\right)^2 - 1\right]$$

$$b_{12} = \frac{\omega\mu_0\beta_1}{k}\left[\left(\frac{P_2}{P_1}\right)^2 \mu_r \tan\beta_1 d - \frac{\beta_2}{\beta_1}\right]$$

$$b_{21} = \frac{\omega K\epsilon_0\beta_1}{k}\left[\left(\frac{P_2}{P_1}\right)^2 \cot\beta_1 d + \frac{1}{K}\frac{\beta_2}{\beta_1}\right]$$

$$\det = b_{11}b_{22} - b_{12}b_{21}$$

$$F_1 = \frac{\omega\mu_r\mu_0\beta_1 \tan\beta_1 d}{P_1^2}.$$

The phase constant k or the quantity ξ can be found by setting the determinant of the coefficients of the unknown current amplitudes I_{x0} and I_{z0} to zero. Because the integrands in the above equations are all quite lengthy, it is quite apparent at this point that the computation time for such a solution will be enormous. A more practical solution is presented in the next section.

B. Solution for Only Longitudinal Current

As mentioned previously, the strip width is usually very small compared to a wavelength so that for the lowest order hybrid mode it suffices to neglect the transverse current and to satisfy (20) and (21) only at the center of the strip $x=0$ instead of over the range $-w/2 \le x \le w/2$. Thus, a single integral equation containing the unknown quantity ξ can be obtained from the coupled pair of integral equations (24) by setting both I_{x0} and x equal to zero and is given by:

$$\int_0^{\infty} \frac{\beta_1 Z I_z(\gamma)}{(YH)^2 + \frac{KZ}{\xi}\lambda_0^2\beta_1\left(Q\cot\beta_1 d - \frac{\beta_2}{K\beta_1}\right)}\, d\gamma = 0 \tag{25}$$

where

$$\gamma = \alpha w; \qquad Q = \frac{\xi - 1}{\mu_r K - \xi};$$

$$Y = \frac{\mu_r K - 1}{\mu_r K - \xi};$$

$$H = \frac{\lambda_0}{w}\gamma; \qquad Z = Q\mu_r \tan\beta_1 d + \frac{\beta_2}{\beta_1};$$

$$I_z(\gamma) = J_0\left(\frac{\gamma}{2}\right).$$

Note that the lower integration limit can be made zero since the integrand is an even function of γ. Also note that the amplitude I_{z0} of the current distribution function is not needed for the solution of ξ; only the part of the Fourier transform that is a function of γ is utilized.

As will be shown later, the alternate expression for the current Fourier transform given by (4) gives better than one-percent accuracy for ξ and, furthermore, requires much less computer time. It is, in fact, the best function to use for microstrip lines having a large w/d ratio. This stems from the fact that the Maxwell current distribution is strictly correct for an isolated conducting strip, i.e., for the case where the ground plane is an infinite distance away from the strip. As the ground plane is brought closer, the ratio w/d increases and the current distribution approaches a more constant distribution across the strip width [19].

IV. Determination of the Characteristic Impedance

For a hybrid mode an exact definition for characteristic impedance does not exist. However, one definition that is used for most other types of transmission lines is given in terms of the power P flowing along the longitudinal direction and of the total current I flowing on the strip:

$$Z_0 = P/I^2. \tag{26}$$

An expression for power is obtained by integrating the z component of the Poynting vector $\boldsymbol{S}=\boldsymbol{E}\times\boldsymbol{H}^*$ over the cross section a' of the microstrip configuration as shown below [11]:

$$P = 1/2 \int\int_{a'} (\boldsymbol{E}\times\boldsymbol{H}^*)\cdot\bar{a}_z\,dx\,dy. \tag{27}$$

The total current is obtained simply by integrating the current distribution $I_z(x)$ across the width of the strip:

$$I = \int_{-w/2}^{w/2} I_z(x)dx. \tag{28}$$

The fact that the microstrip line is an open structure makes the computation of the above expression very lengthy. This computation is hardly justified at the present time since the experimental microstrip impedance determinations require an accuracy beyond the limit of available measurement techniques. Therefore, the following TEM-like expression for impedance in terms of the dispersive parameters of phase velocity and effective dielectric constant is probably adequate over a frequency range in which the dispersion remains only a few percent:

$$Z_0 = \frac{1}{vC} = \frac{\mu_{\mathrm{eff}}}{\sqrt{\xi}} Z_0\big|_{K=1} \tag{29}$$

where

$$C = \epsilon_{\mathrm{eff}} C_0 = \text{capacitance/unit length}$$

$$C_0 = C \quad \text{for } K=1,\ \mu_r = 1$$

$$v = \frac{v_0}{\sqrt{\xi}}$$

$$Z_0\big|_{K=1} = \frac{1}{v_0 C_0} = \text{characteristic impedance of air microstrip line.}$$

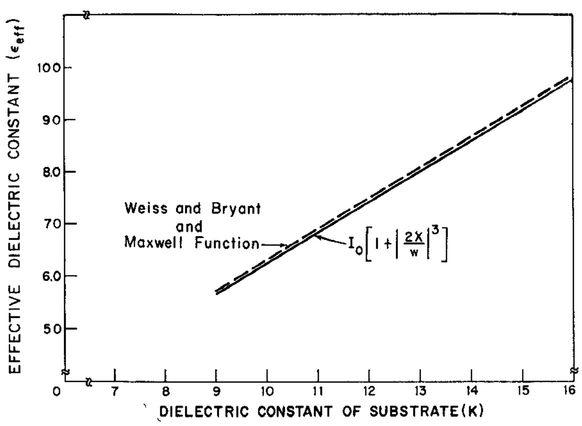

Fig. 4. Effective dielectric constant versus K: $w/d=0.40$. Note: Percentage difference between computed values (solid curve) and those obtained by Weiss and Bryant (dashed curve) is less than one percent.

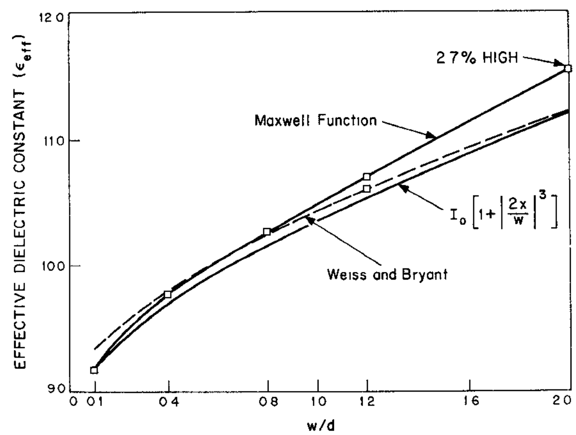

Fig. 5. Effective dielectric constant versus w/d: $K=16$.

The effective value of permeability μ_{eff} and the normalized propagation constant $k/k_0=\sqrt{\xi}$ are frequency-dependent quantities obtained from the integral equation (25) while $Z_0|_{K=1}$ may be obtained from Wheeler's theory [1].

V. Presentation and Discussion of Theoretical and Experimental Results

Using a digital computer to solve integral equation (25) for the quantity ξ, it was only necessary to sum over values of the integration variable γ between 0 and 100 in order to acquire accuracy to within the fourth decimal place because the integrand converged quite rapidly. A half-interval search technique [20] was used to find the root of the equation. It found the value of ξ that makes the left-hand side of (25) less than 10^{-5}.

A. Single Microstrip Line on a Dielectric Substrate

In order to establish the validity of the theory, it was necessary to initially make a comparison with the quasi-static solutions of Bryant and Weiss [3] by solving for $\xi=\epsilon_{\mathrm{eff}}$ at zero frequency. Longitudinal current solutions were obtained using the Fourier transforms for both current distributions given by (2) and (4), and the results were plotted as functions of K and w/d, as shown by Figs. 4 and 5, respectively. The first curve, which was

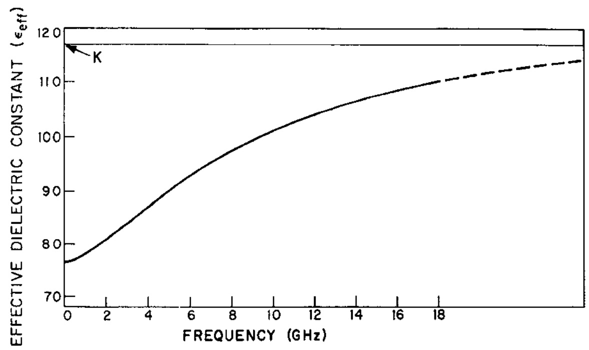

Fig. 6. Effective dielectric constant versus frequency. $K=11.7$; $w/d=0.96$; $d=0.317$ cm.

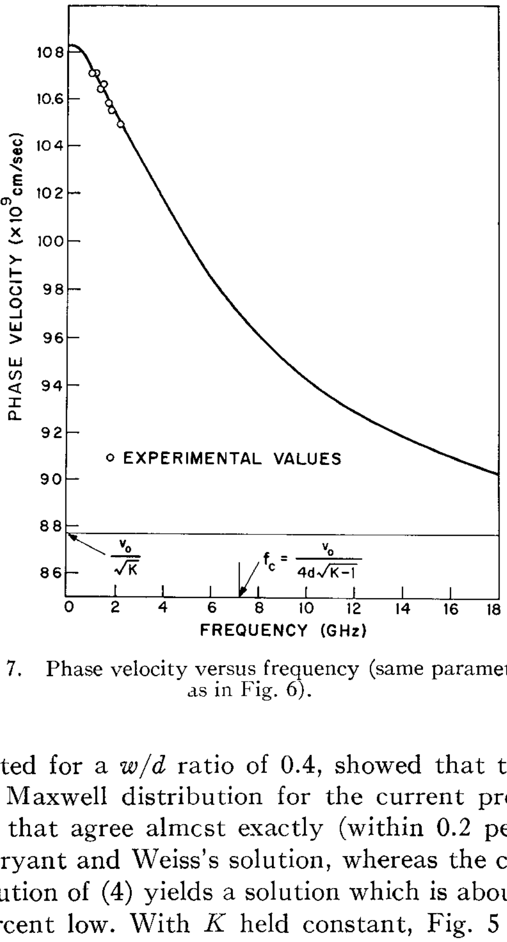

Fig. 7. Phase velocity versus frequency (same parameters as in Fig. 6).

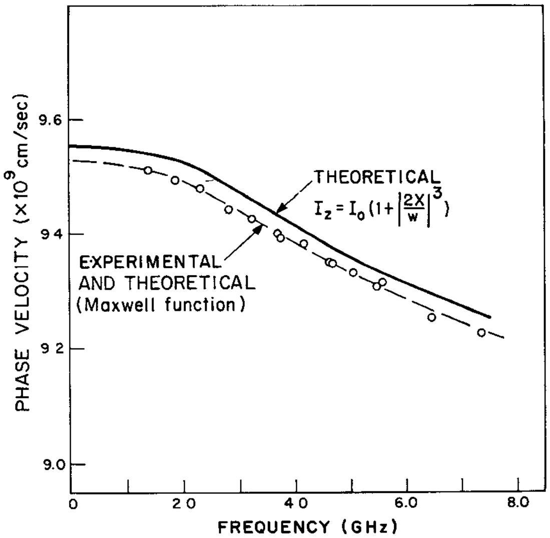

Fig. 8. Theoretical and experimental curves of phase velocity versus frequency: $K=15.87$; $w/d=0.543$; $d=0.1016$ cm. Note: Percent difference between experimental and theoretical curves is σ constant 0.3 percent for the least accurate current distribution.

calculated for a w/d ratio of 0.4, showed that the use of the Maxwell distribution for the current produces results that agree almcst exactly (within 0.2 percent) with Bryant and Weiss's solution, whereas the current distribution of (4) yields a solution which is about 0.6–0.8 percent low. With K held constant, Fig. 5 shows that the solution utilizing the Maxwell function agrees best with the recent quasi-static solutions mentioned in Section I for w/d values in the range $0<w/d\leq 1.2$, while the current distribution function of (4) yields better agreement for higher w/d values ($w/d>1.2$). If the least amount of computer time is desired, then the use of the latter function, which is accurate to better than one percent for all values of w/d and K, is recommended.

The complete solution obtained from the coupled pair of integral equations involving both components of current required a large amount of computer time. Several points were computed and the results were in excellent agreement with the longitudinal current solution both at zero frequency and at a finite frequency. It was concluded that the solution which neglects the transverse current is a very good approximation as long as the normalized strip width w/λ is less than about 0.1.

Returning to (25) and solving for $\xi=\epsilon_{eff}$ as a function of frequency results in a dispersion curve, illustrated by Fig. 6. Even though the extent of the theoretical plot is beyond the frequency range over which the transverse current can be neglected, the shape of the curve checks with the results of Hartwig *et al.* [21]. The effective dielectric constant asymptotically approaches K at very high frequencies, indicating that all the energy is being confined to the dielectric. Since the hybrid-mode solution is a superposition of an infinite number of surface waves, this result is expected. The phase velocity v can now be obtained from (19); its frequency dependence is shown in Fig. 7. It is interesting to note the relative position of the divergence frequency f_c for the TE_1 surface wave, which is given by the following equation:

$$f_c = \frac{v_0}{4d\sqrt{K-1}}. \tag{30}$$

It appears to occur very close to the inflection point of the phase velocity curve. In practice, use of microstrip should be restricted to frequencies below f_c in order to avoid excitation of surface waves that will propagate away from the strip.

An experimental check of the above frequency dependence of velocity can easily be accomplished by the use of a microstrip resonator which is in the form of a ring [22] or a straight open-ended line. The former is employed whenever end effects associated with the straight-line resonator become significant. The results of velocity measurements along with theoretical curves are shown in Fig. 8 for a 50 ω microstrip line deposited by vacuum-deposition techniques onto a very commonly used magnesium titanate substrate.[1] The dielec-

[1] Material made by Trans-Tech, Inc., Gaithersburg, Md.

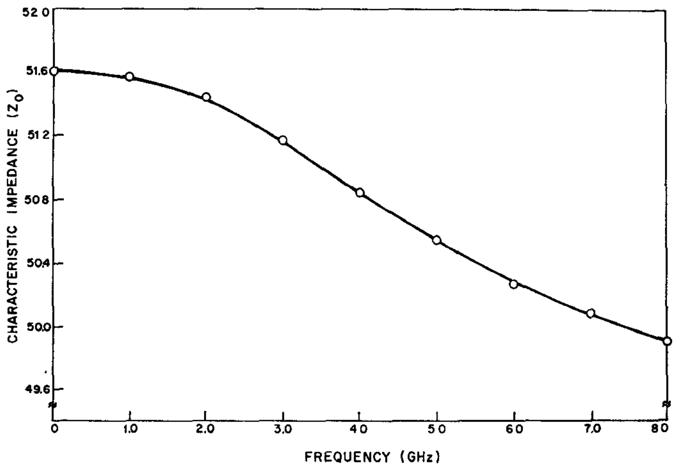

Fig. 9. Characteristic impedance versus frequency (same parameters as in Fig. 8).

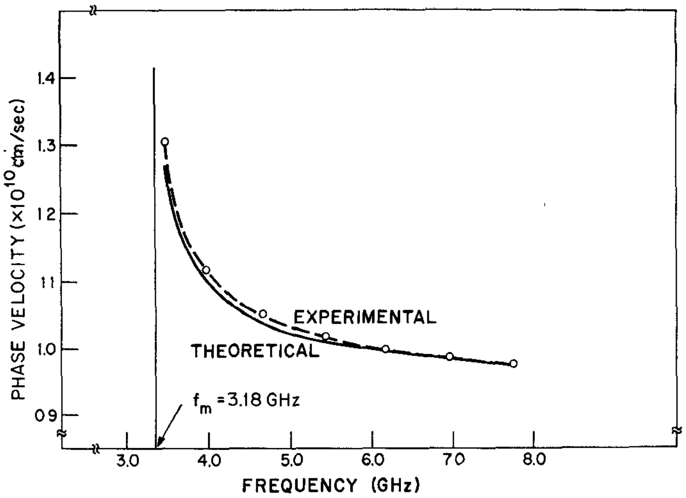

Fig. 10. Demagnetized ferrite microstrip phase velocity versus frequency: $K=15.5$; $w/d=0.431$; $d=0.074$ cm; $4\pi M_s=1.210$ kG.

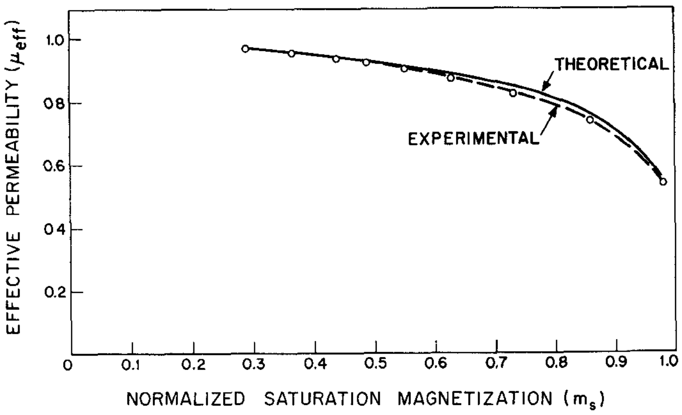

Fig. 11. Demagnetized ferrite microstrip effective permeability versus normalized saturation magnetization (same parameters as in Fig. 10).

tric constant of a sample of this material was accurately measured by Courtney of M.I.T. Lincoln Laboratory, using a precise TE_{01} cavity technique [23]. Since the substrate's dielectric constant was large and its thickness small, no significant fringing at the end of the straight-line resonator would be expected [18]. However, as a check, two different lengths of line were used in the measurement and the velocities compared. Negligible difference was observed. In comparing the above results with the theory, there is extremely good agreement if the Maxwell current distribution is used in the integral equation (25). The other distribution (4) produces an inaccuracy of only about 0.3 percent while requiring one-fifth as much computer time as the Maxwell function.

Using the values of effective dielectric constant versus frequency obtained from the above calculations, (29) was used to get the variation of characteristic impedance with frequency. The theoretical curve is given in Fig. 9 and shows a total impedance change of only three percent at 8 GHz.

B. Single Microstrip Line on a Demagnetized Ferrite Substrate

For the demagnetized ferrite case, integral equation (25) is again used to obtain $\xi=\mu_{eff}\epsilon_{eff}$. The expression for the ferrite's scalar permeability, which must be substituted into the integral equation, is a function of the material's saturation magnetization $4\pi M_s$ (in kilogauss) and the frequency [24] f (in gigahertz):

$$\mu_r = \frac{2}{3}(1 - m_s^2)^{1/2} + \frac{1}{3} \tag{31}$$

where m_s is known as the normalized saturation magnetization and is given by

$$m_s = \frac{2.8(4\pi M_s)}{f}$$

with the factor 2.8 being the gyromagnetic ratio in units of GHz/kG. With the use of (19), a theoretical curve of ferrite microstrip phase velocity versus frequency can be obtained with $4\pi M_s$, K, w/d, and d as parameters. Fig. 10 shows such a curve for a microstrip on a Trans-Tech G-1001 garnet substrate. As the permeability of the material decreases rapidly near the natural resonant frequency $f_m=2.8(4\pi M_s)$, the phase velocity increases at a fast rate. Experimental measurements obtained with a ring resonator given in the same figure show good agreement with the theoretical results.

A normalized curve that is useful for all ferrite substrates with the same geometrical parameters and dielectric constant is that of effective permeability μ_{eff} versus normalized saturation magnetization m_s. Such a curve can be derived by using the quantity ξ calculated above as well as an ϵ_{eff} that is a solution of the integral equation for a pure dielectric substrate having the same values of K, w/d, and d as the ferrite. Then μ_{eff} will be simply given by

$$\mu_{eff} = \frac{\xi}{\epsilon_{eff}\big|_{\text{dielectric}}}. \tag{32}$$

Fig. 11 shows the results of this calculation along with experimental values. It has been experimentally verified by the author at M.I.T. Lincoln Laboratory that microstrip lines with frequently used ferrite materials having saturation magnetizations between 400 G and 1400 G obey this same μ_{eff} versus m_s curve.

VI. Conclusion

A frequency-dependent solution has been presented for microstrip on both a dielectric and a demagnetized ferrite substrate. It utilizes a Fourier transform method that sums up the solutions for a fictitious surface current distribution in order to obtain the fields that are caused by the actual current distribution that is finite only over the region occupied by the conducting strip. Due to the fact that the transverse current is expected to be much smaller in amplitude than the longitudinal current for normal operating frequencies and strip widths, a solution involving only the longitudinal current was found to be sufficiently accurate. This has been demonstrated by the excellent agreement obtained between theoretical and experimental values of phase velocity over a wide frequency range.

Two interesting theoretical results obtained from the study of frequency-dependent behavior of microstrip lines are 1) the dispersion curve has an inflection point which is a function of the substrate's thickness d, dielectric constant K, and velocity of light v_0 according to the equation $f_c = v_0/(4d\sqrt{K-1})$; and 2) at very high frequencies the effective dielectric constant asymptotically approaches the substrate's dielectric constant K and the phase velocity approaches $v_0/\sqrt{K}$, which indicates an increasing part of the energy is being confined to the dielectric. However, the coupling to surface waves and the increasing importance of radiation near and above f_c prevent accurate experimental verification of theoretical results. For these high frequencies the most accurate analysis should include the contribution of the transverse current and the higher order modes.

Appendix

Microstrip Current Distribution

This appendix gives a derivation of the expressions (1) and (6) for the longitudinal and transverse components of current, respectively.

A. Longitudinal Current

An expression for the charge density distribution on an isolated conducting strip was derived by Maxwell [16]. For the dynamic case, it applies to the TEM solution for the longitudinal surface current distribution on a microstrip line as long as the ground plane is spaced far enough away from the strip. As shown in Section V, this restriction corresponds to keeping the w/d values less than about 1.2. Because the circuit dimensions are very small compared to a wavelength, we assume this treatment to be quasi-static in nature and thus the hybrid-mode current distribution is taken to be the same as that for a pure TEM mode. This assumption is borne out by the extremely good agreement between theoretical and experimental results. Since this good agreement extends up to very high frequencies (at least 8 GHz), the skin effect, which would draw the current distribution even further to the edges of the strip with increasing frequency [25], must be a second-order effect. The Maxwell distribution approaches infinity at the strip's edge anyway, so that the form of the distribution remains consistent with the skin effect.

Maxwell considered an isolated conducting strip on which a charge of 1 C/m was placed. He used a conformal transformation to find how this charge distributes itself across the strip. The following function for the surface charge density $\sigma(x)$ results:

$$\sigma(x) = \frac{1}{\pi\sqrt{1-x^2}}, \qquad -1 \le x \le 1. \tag{33}$$

If the strip width is w instead of 2 and the total charge on the strip is σ_0 instead of 1, then the surface charge distribution becomes

$$\sigma(x) = \frac{\sigma_0}{\pi\sqrt{1-(2x/w)^2}}, \qquad -w/2 \le x \le w/2. \tag{34}$$

The approximate expression for the longitudinal current is $I_z(x) \cong v\sigma(x)$, where v is the phase velocity.

B. Transverse Current

The transverse current distribution can be obtained by using the continuity equation

$$\frac{\partial I_z}{\partial_z} + \frac{\partial I_x}{\partial_x} = -j\omega\sigma(x). \tag{35}$$

In the quasi-TEM-mode approximation, the following expression relates the longitudinal current to the charge density distribution $\sigma_a(x)$ without the substrate, which has been scaled up in the ratio of the total charges [14] $\sigma_{T\,\text{dielectric}}$, $\sigma_{T\,\text{air}}$:

$$I_z(x) = vc\sigma_a(x)e^{-jkz}, \qquad c = \frac{\sigma_{T\,\text{dielectric}}}{\sigma_{T\,\text{air}}}. \tag{36}$$

Thus, (35) becomes

$$\begin{aligned}\frac{\partial I_x}{\partial_x} &= -j\omega\sigma(x) + jkvc\sigma_a(x)\\ &= -j\omega[\sigma(x) - c\sigma_a(x)].\end{aligned} \tag{37}$$

For the microstrip's lowest order mode, $I_x(x)$ is zero at the center of the strip and has odd symmetry about this point. Therefore, the expression for $I_x(x)$ is the following:

$$I_x(x) = -j\omega\,(\operatorname{sgn} x)\int_0^x [\sigma(x) - c\sigma_a(x)]dx, \qquad |x| \le w/2 \tag{38}$$

where

$$\begin{aligned}\operatorname{sgn} x &= -1, \qquad x < 0\\ &= +1, \qquad x > 0.\end{aligned}$$

Upon substituting charge distribution data from Bryant and Weiss's solution [3], it was found that the form of the distribution can be described by (6), and its magnitude is proportional to the normalized strip width w/λ. For values of $w/\lambda < 0.1$, the average transverse current amplitude across one-half the strip width is less than ten percent of the average longitudinal current amplitude.

Acknowledgment

The author wishes to thank his dissertation advisor, Dr. N. Farhat of the University of Pennsylvania for his contribution; C. Blake and D. Temme of Lincoln Laboratory for their support; T. G. Bryant for permission to use his Green's function method results; and Mrs. Janet Reid for her valuable instruction and assistance in programming and using the CP/CMS time-sharing computer system.

References

[1] H. A. Wheeler, "Transmission-line properties of parallel strips separated by a dielectric sheet," *IEEE Trans. Microwave Theory Tech.*, vol. MTT-13, Mar. 1965, pp. 172–185.

[2] P. Silvester, "TEM wave properties of microstrip transmission lines," *Proc. Inst. Elec. Eng.*, vol. 115, Jan. 1968, pp. 43–48.

[3] T. G. Bryant and J. A. Weiss, "Parameters of microstrip transmission lines and of coupled pairs of microstrip lines," *IEEE Trans. Microwave Theory Tech.*, vol. MTT-16, Dec. 1968, pp. 1021–1027.

[4] H. E. Green, "The numerical solution of some important transmission line problems," *IEEE Trans. Microwave Theory Tech.*, vol. MTT-13, Sept. 1965, pp. 676–692.

[5] H. E. Stinehelfer, Sr., "An accurate calculation of uniform microstrip transmission lines," *IEEE Trans. Microwave Theory Tech.*, vol. MTT-16, July 1968, pp. 439–444.

[6] E. Yamashita, "Variational method for the analysis of microstrip-like transmission lines," *IEEE Trans. Microwave Theory Tech.*, vol. MTT-16, Aug. 1968, pp. 529–535.

[7] G. I. Zysman and D. Varon, "Wave propagation in microstrip transmission lines," *1969 IEEE Int. Microwave Symp. Dig.*, pp. 3–9.

[8] J. S. Hornsby and A. Gopinath, "Numerical Analysis of a dielectric-loaded waveguide with a microstrip line—Finite difference methods," *IEEE Trans. Microwave Theory Tech.*, vol. MTT-17, Sept. 1969, pp. 684–690.

[9] ——, "Fourier analysis of a dielectric-loaded waveguide with a microstrip line," *Electron. Lett.*, vol. 5, June 12, 1969, pp. 265–267.

[10] J. Brown, "The types of waves which may exist near a guiding structure," *Proc. Inst. Elec. Eng.*, vol. 100, p. 3, Nov. 1953, pp. 363–364.

[11] R. E. Collin, *Field Theory of Guided Waves.* New York: McGraw-Hill, 1960, pp. 10, 170–174, 484–485.

[12] G. Goubau, "On the excitation of surface waves," *Proc. IRE*, vol. 40, July 1952, pp. 865–868.

[13] M. Schetzen, "Printed microwave systems," M.S. thesis, Dep. Elec. Eng., Massachusetts Institute of Technology, Cambridge, 1954.

[14] A. Gopinath, R. Horton, and B. Easter, "Microstrip loss calculations," *Electron. Lett.*, vol. 6, Jan. 22, 1970, pp. 40–41.

[15] T. Kaneki, "Analysis of linear microstrip using an arbitrary ferromagnetic substance as the substrate," *Electron. Lett.*, vol. 5, Sept. 18, 1969., pp. 463–465.

[16] J. C. Maxwell, *A Treatise on Electricity and Magnetism*, 3rd ed., vol. 1. New York: Dover, 1954, pp. 296–297.

[17] J. A. Stratton, *Electromagnetic Theory.* New York: McGraw-Hill, 1941, pp. 349–351.

[18] E. J. Denlinger, "Radiation from microstrip resonators," *IEEE Trans. Microwave Theory Tech.*, vol. MTT-17, Apr. 1969, pp. 235–236.

[19] M. E. Hellman and J. Palocz, "The effect of neighboring conductors on the currents and fields in plane parallel transmission lines," *IEEE Trans. Microwave Theory Tech.*, vol. MTT-17, May 1969, pp. 254–259.

[20] S. Kuo, *Numerical Methods and Computers.* Reading, Mass.: Addison-Wesley, 1965, pp. 83–87.

[21] C. P. Hartwig, D. Massé, and R. A. Pucel, "Frequency dependent behavior of microstrip," *1968 Int. Symp. Dig.*, pp. 110–116.

[22] P. Troughton, "Measurement techniques in microstrip," *Electron. Lett.*, vol. 5, Jan. 23, 1969, pp. 25–26.

[23] W. Courtney, "Analysis and evaluation of a method of measuring the complex permittivity and permeability of microwave insulators," to be published in *IEEE Trans. Microwave Theory Tech.*, vol. MTT-18, Aug. 1970, pp. 476–485.

[24] E. Schlömann, J. Green, F. Sandy, and J. Saunders, "Characterization of the microwave tensor permeability of partially magnetized materials," RADC-TR-69-93, vol. 3, Feb. 1969, pp. 33–71.

[25] P. Silvester. *Modern Electromagnetic Fields.* Englewood Cliffs, N. J.: Prentice-Hall, 1968, pp. 235–238.